Mineralium Deposita (2002) 37: 421–432
DOI 10.1007/s00126-001-0222-y

ARTICLE

**Michel Jébrak · Pablo L. Higueras**
**Éric Marcoux · Saturnino Lorenzo**

# Geology and geochemistry of high-grade, volcanic rock-hosted, mercury mineralisation in the Nuevo Entredicho deposit, Almadén district, Spain

Received: 5 September 2001 / Accepted: 12 September 2001 / Published online: 2 February 2002


**Abstract** The Nuevo Entredicho deposit contains the richest concentration of mercury in the Almadén district, locally grading as much as 45% Hg. This ore deposit is hosted within an alkaline, conically shaped diatreme, about 150 m in diameter, which was subsequently filled with phreatomagmatic breccias. The diatreme cuts an Ordovician to Silurian clastic sedimentary rock sequence that is intercalated with basaltic sills. Structural analysis reveals a complex tectonic history with three main phases of Hercynian deformation. Mineralisation occurs as cinnabar replacements in volcanic tuffs and breccias and as recrystallised veins in tensions cracks associated with pyrophyllite and hydrothermal pyrite, which is strongly enriched in Cu, Pb and Hg. Lead isotopes in pyrite are characterised by high $^{207}Pb/^{204}Pb$ ratios (15.70–15.75), suggesting a contribution of ancient upper continental crust remobilised by Silurian–Devonian volcanism, with no mantle involvement. Sulphur isotopes of epigenetic cinnabar and pyrite range from +10.3 to +10.8‰ and from +10.6 to +11.9‰ respectively, suggesting a uniform sulphur source or a constant mixing ratio in the ore fluids. These isotopic compositions differ from those measured in the syngenetic deposits of the Almadén district; they suggest a higher temperature of ore formation of about 300 °C, and a genesis related to a distinct hydrothermal flow path at the Nuevo Entredicho deposit. Deposition of anomalously high-grade mercury ore at Nuevo Entredicho is related to a combination of (1) an abundance of black shale that provided sulphur and increasingly reducing conditions with high sulphide/sulphate ratios, (2) explosive Silurian–Devonian mafic magmatism that provided an initial source of mercury, (3) tectonic activity that lead to structurally favourable sites for ore deposition, and (4) replacement of secondary, carbonate-rich volcanic rocks.

**Keywords** Almadén · Cinnabar · Epigenetic mineralisation · Stable isotope · Volcanic-hosted

Editorial handling: G. Beaudoin

M. Jébrak (✉)
Université du Québec à Montréal,
Département des Sciences de la Terre,
C.P.8888, Succ. Centre-Ville,
Montréal (Qc), H3C 3P8 Canada
E-mail: jebrak.michel@uqam.ca

P.L. Higueras
Universidad de Castilla La Mancha,
Dept Ingenieria Geologica y Minera,
13400 Almadén, Ciudad Real, Spain

É. Marcoux
Université d'Orléans, Département des Géosciences,
ISTO, UFR Sciences, 45072 Orléans Cedex 2, France

S. Lorenzo
Minas de Almadén y Arrayanes
S.A. Cerco de San Teodoro s/n,
13400 Almadén (Ciudad Real), Spain

## Introduction

The Almadén district is the largest mercury producer in the world and accounts for more than one-third of the total world output. The cinnabar deposits show a strong spatial association with the Criadero quartzite unit of Ordovician–Silurian age (Prado 1855; Saupé 1990; Villas et al. 1999), yet the equivocal nature of the genetic relationship between mineralisation and epicontinental clastic sedimentation has long presented a challenge to developing a genetic model for the mineralisation. Although a connection with magmatic rocks was proposed long ago (Van der Veen 1924), it wasn't until the 1980s that high grade mercury concentrations were found in association with volcanoclastic alkaline rocks (Hernandez 1984). Mercury production from an igneous rock-hosted deposit commenced in 1986 at Las Cuevas (Fig. 1). The ore has since been interpreted as the product of tectonic remobilisation from early stratabound mineralisation in the Criadero quartzite (Jébrak and Hernandez 1995, 1997; Ortega 1997), possibly because of movement along a shear zone (Palero 1997).

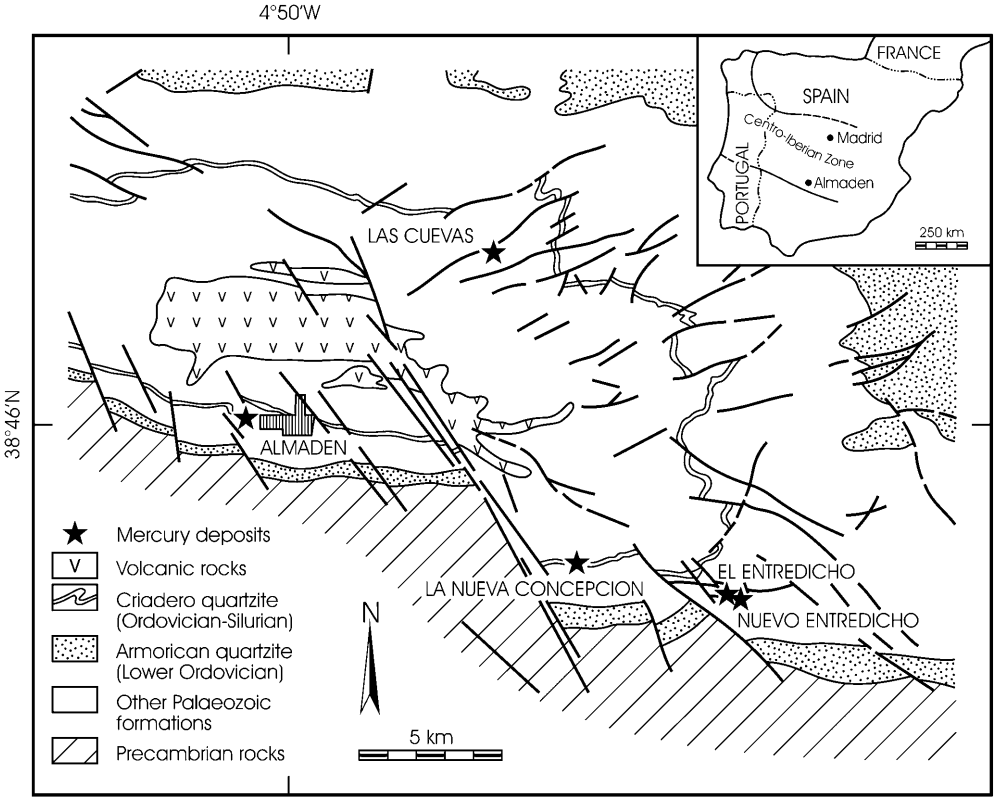


**Fig. 1** Regional geological map of the Almadén mercury district including location of the Las Cuevas, El Entredicho, Almadén and Nuevo Entredicho deposits

In 1985, a drilling campaign near the El Entredicho deposit intersected the high-grade, dominantly volcanic rock-hosted mineralisation of Nuevo Entredicho. Grades as high as 45.81% Hg over 1.84 m (true thickness) represent some of the richest mercury concentrations ever drilled in the world. Calculated reserves of this small deposit total about 15,500 t, with an average grade of 17.5% Hg. This paper describes the geological environment of the Nuevo Entredicho deposit, together with new geochemical and isotopic data, which permit a better understanding of the cause and significance of grade variations in the Almadén district.

## Geology

The Almadén district is located 300 km south of Madrid on the Iberian Peninsula and forms part of the Centro-Iberian Zone of the Hercynian chain (Julivert et al. 1972; Dallmeyer and Martinez Garcia 1990; Fig. 1). Three cycles of sedimentation have been distinguished: Late Precambrian, Palaeozoic and Late Cenozoic. Mercury ores in the Almadén district are concentrated exclusively in Palaeozoic rocks. These rocks formed during lower Palaeozoic epicontinental marine sedimentation on a stable platform and were subjected to a main episode of deformation and low-grade metamorphism during the Carboniferous.

A large synclinorium occurs in Palaeozoic rocks overlying the Precambrian basement. The Palaeozoic sequence is a 2,700- to 4,000-m-thick detrital suite of quartz–arenites, rhythmically interlayered sandstones and shales, and black shales, with minor horizons of carbonate, volcanic and volcaniclastic rocks (Saupé 1973; Garcia Sansegundo et al. 1987). Four major units of quartzite have been recognised; the Armorican quartzite (Lower Ordovician), the Canteras quartzite (Middle to Upper Ordovician), the Criadero quartzite (Upper Ordovician–Lower Silurian) and the Base quartzite (Lower Devonian). The Hirnantian–Llandoverian Criadero quartzite unit is the main host to mercury mineralisation. Sedimentary rocks of Devonian age are composed of sandstone, shale and lenses of fossil-rich carbonate rocks, all of which were deposited under conditions similar to those of the Ordovician rocks. Upper Carboniferous rocks near the synclinorium axis discordantly overly Devonian rocks.

The Almadén Synclinorium contains diverse types of magmatic rocks (Higueras et al. 2000), including basaltic sills (both porphyritic and doleritic), and diatremes (brecciated rocks, locally called Frailesca). These rocks are present throughout the stratigraphic succession, but are especially abundant in Silurian to Devonian sequences. The Criadero quartzite is intruded by both types of magmatic rocks. Diatremes cut the stratigraphic units at a slight angle in most of the mercury mines, and have a conical shape with a maximum diameter of several hundred metres. Saupé (1990) proposed that the diatreme magmatism was contemporaneous with sedimentation and, therefore, may represent shallow submarine phreatomagmatic eruptions. The original magmas may have been derived from a garnet–lherzolite mantle source enriched in incompatible elements and related to an intra-plate mantle plume during lower Palaeozoic times (Higueras and Munhá 1993; Higueras et al. 2000).

Three episodes of Hercynian deformation have been recognised in the Almadén Synclinorium (Saupé 1973, 1990; Hernandez 1984; Garcia Sansegundo et al. 1987). The initial major phase of folding during homogeneous NNE–SSW shortening resulted in a narrow elongate synclinorium orientated 100–110°N, with an estimated age of $335 \pm 15$ Ma (Nägler et al. 1992). Related folds have subvertical axial planes, subhorizontal axes and inconspicuous axial plane schistosities. Reverse faults are commonly associated with folding and are better developed in the southern limb. A second phase of heterogeneous E–W shortening caused rotation of the previous folds along discrete shear zones. Deformation was concentrated along two conjugate systems of predominantly brittle shear bands oriented NW–SE (sinistral) and ENE–WSW (dextral). Finally, a late N–S-shortening event created conjugate sets of

NNW–SSE- and NNE–SSW-oriented faults and caused reactivation of earlier structures.

The entire sedimentary pile has been weakly metamorphosed to the pumpellyite facies (Saupé 1973; Higueras 1995). Illite associated with argillic alteration from the Las Cuevas and El Entredicho deposits provided an $^{40}Ar/^{39}Ar$ age of $361 \pm 2$ Ma (Hall et al. 1997), which corresponds to the end of Frasnian time. New $^{87}Sr/^{86}Sr$ data give a model age of $365 \pm 17$ Ma (Higueras et al. 2001), consistent with the argon age. Two interpretations have been proposed for this intermediate age between syn-sedimentary volcanic activity and Hercynian deformation: (1) the age corresponds to isotopic resetting either by metamorphism during tectonic events that affected the Iberian Peninsula (Shelley and Bossiere 2000) or (2) the age represents long-lasting submarine magmatic activity that persisted during most of Silurian and Devonian time (Higueras et al. 2001). Taking into account that deformation and metamorphism in this part of the Iberian Massif is younger (~300 Ma), we envisage the second hypothesis as the most probable, although we caution that further geochronological work is needed to clarify the thermal evolution of the area.

## Local geology of the Nuevo Entredicho deposit

### Sedimentary rocks

The El Entredicho area, which includes the Nuevo Entredicho deposit, is located in the easternmost part of the Almadén Synclinorium (Figs. 1, 2). The sedimentary pile comprises six divisions (from bottom to top; Hernandez 1984; Gallardo et al. 1994): (1) dark-coloured and fine-grained shale, with narrow sandstone interbeddings, cut by numerous thin basaltic dikes (Pizarras de Muro = 'footwall shales'); (2) the lower Criadero quartzite unit (averages 1 m thick); (3) intermediate shales (averages 5 m thick); (4) a basaltic sill 2 to 5 m thick, containing ultramafic enclaves of altered olivine, orthopyroxene, minor plagioclase and unaltered Cr-spinel; (5) upper Criadero quartzite unit (averages 45 m thick) consisting of interlayered shales and sandstones that display numerous sedimentary structures and grading into dark sandstones and quartzites in the upper levels; and (6) hanging wall black shales and basaltic lavas.

### Diatreme

The sedimentary sequence is cut by a diatreme filled with Frailesca that includes volcanoclastic rocks, flow basalt and epiclastic breccias (Figs. 2 and 3). The diatreme is approximately 150 m in diameter at the surface, and has been identified in drill cores to a depth of at least 210 m, transecting progressively older rocks (Fig. 4A). The open conical shape suggests emplacement in unconsolidated rocks, similar to the Argyle lamproite pipe in Western Australia (Boxer and Jaques 1990). The diatreme may be close in age to Criadero quartzite sedimentation. The diatreme shows units from several volcanic episodes: an early phreatomagmatic breccia, a flow of vesicle-rich olivine-basalt, a chaotic breccia and rocks from a late volcaniclastic eruption. All these components display numerous facies changes.

The oldest unit in the diatreme is composed of a black shale interbedded with thin horizons of fragmented volcanic and sedimentary rocks. Sedimentary clasts are dominant, and as large as 20 cm in diameter. Accretionary lapilli and bomb-impact sag structures in ash are characteristic of aerial transport during eruption and deposition in a water-rich environment (Cas 1989). This episode may, therefore, correspond to a shallow submarine phreatomagmatic breccia event.

The overlying basaltic flow unit is composed of olivine and pyroxene crystals in a feldspathic matrix. Numerous variolitic cavities indicate that the rock was rich in volatiles. Some of the cavities were filled with quartz and carbonate minerals. Blocks containing these cavities were subsequently dismembered and redeposited in the crater and now show an inversed geopetal structure. The top of the flow is marked by a cooling breccia containing devitrified glass. This indicates that the magma was able to reach the surface without interaction with ground water, possibly because congealed lava lined the conduit and acted as a seal.

Chaotic breccias are mainly developed at the northern end of the crater and are characterised by heterolithic blocks that range in size from centimetres to several metres. Fragments of older black shale, lapilli tuffs, basalt and quartzite are contained within the black shale (Fig. 4B). Coarse lithic blocks suggest a proximal source, and the breccias evolve vertically toward finer facies, including cinder-type tuffs with a graphitic matrix. Fragments are affected by quartz–carbonate alteration. The breccias may have developed during the collapse of the maar rim into the crater. This collapse was contemporaneous with deposition of the Criadero quartzite.

Fine-grained pyroclastic tuffs with numerous graphitic shale fragments are interlayered with lava and tuffs. The unit comprises clasts of highly vesicular volcanites, with remnants of olivine and plagioclase phenocrysts. Some rare clasts of siliceous chlorite-bearing sediments have been observed. Intense and pervasive carbonate-rich early alteration of this unit caused it to act as an impermeable barrier, as indicated by numerous hydraulic tension cracks. This Frailesca may be of local origin or related to another eruptive centre.

Bedded to massive polymictic pyroclastic tuffs are also present in the sequence and contain abundant fragments, as large as 10 cm in diameter, of basalt and lesser amounts of black shale and tuff. Inverse graded bedding has been observed. Several horizons are composed of highly vesicular, heterometric, volcanic material and detrital quartz in a silica–chlorite matrix.

The crater represents an explosive eruptive centre. The form of the crater is that of a tuff cone, with steep, inwardly-dipping beds dominated by juvenile magmatic tephra and lithic fragments. Tuff cones commonly form where erupting vents are covered by water. The absence of pillow lava in the basalt flow may signify a short period of emergence or a highly fluid submarine flow. This environment appears similar to that of the modern tuff cone on the volcanic island of Surtsey, which formed

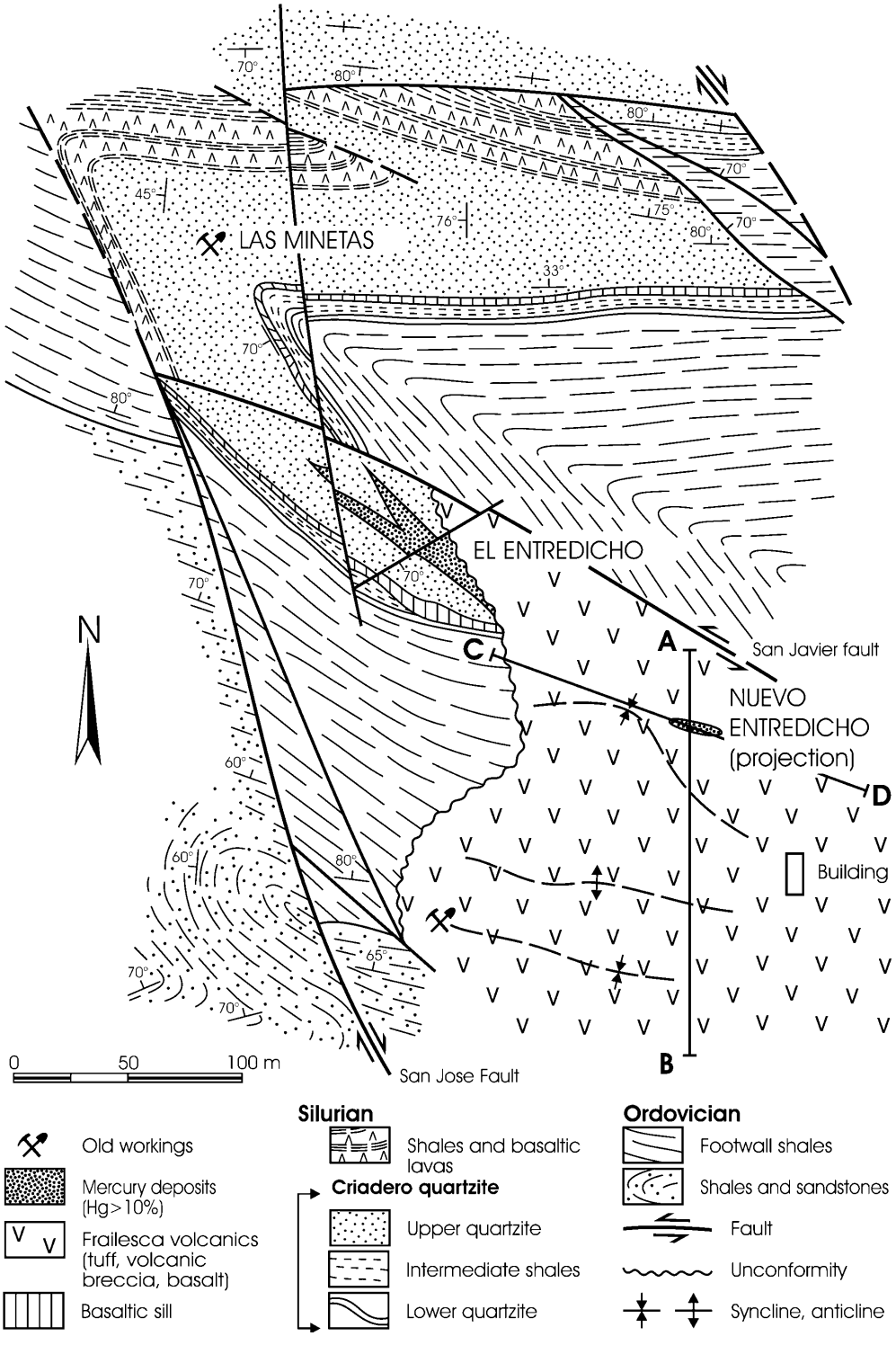


**Fig. 2** Geological map of the El Entredicho area. Projection of the Nuevo Entredicho deposit is shown

in shallow marine waters (130 m deep) off the coast of Iceland between 1963 and 1967 (Thorarinsson 1967). Another well-known ancient example, the Joya Honda maar in Mexico, displays the same type of pyroclastic sequence in black shales, with rapid facies variations (Aranda-Gómez and Luhr 1996). Brecciation is associated with subsidence and slumping of unconsolidated partly water-saturated beds during accumulation of material within the maar. Elevated fluid pressure at the end of the eruption is indicated by hydraulic breccias, highly vesicular volcanic rocks and intense carbonate alteration. The observed facies evolution indicates that high fluid pressure existed early during the eruptive cycle. Carbon-dioxide-rich hydrothermal fluids were exsolved from the cooling basalt as indicated by carbonate alteration of the volcanic pile.

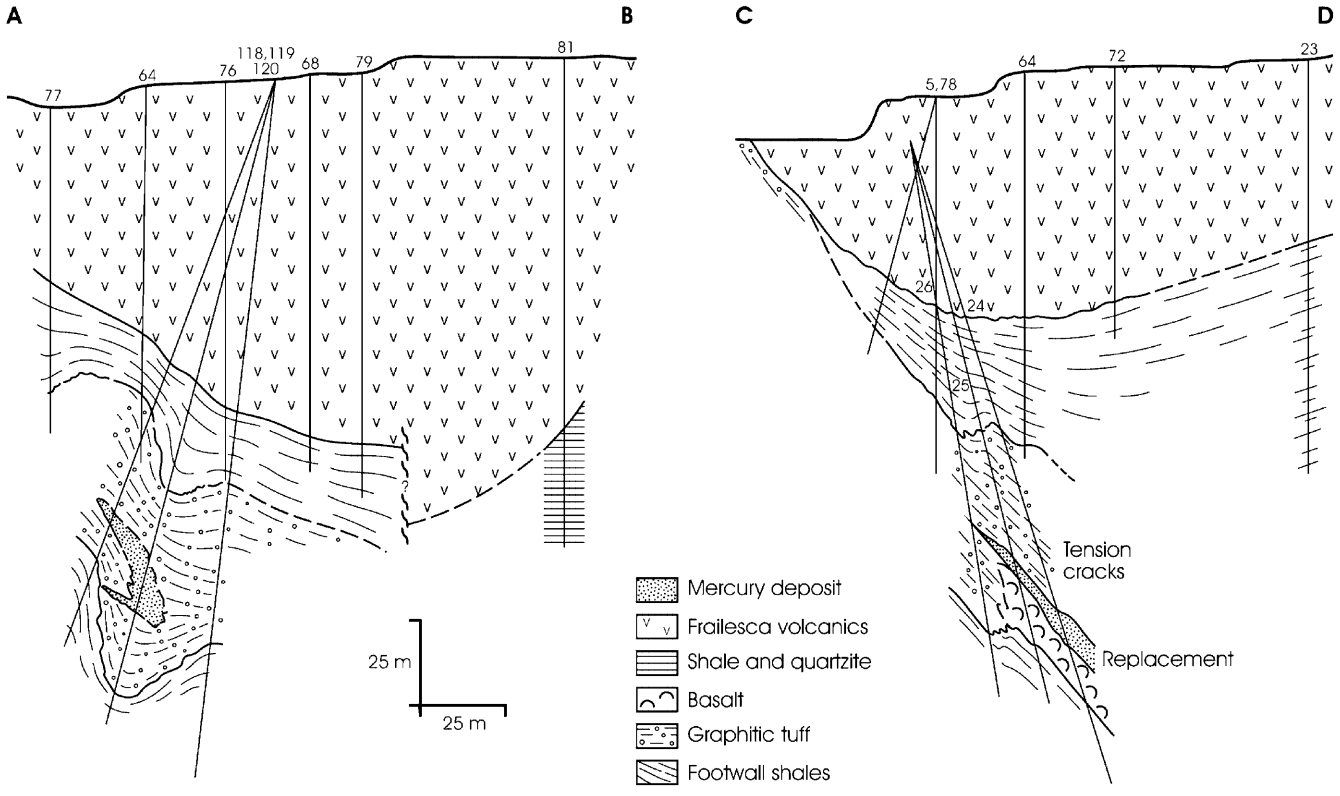


**Fig. 3** Cross sections through the Nuevo Entredicho mercury deposit

## Structural history

The El Entredicho area is located in a zone of tight synclinal folding in the easternmost part of the regional Almadén Synclinorium. Structural studies reveal a complex tectonic history characterised by three main phases of Hercynian deformation.

An initial phase of folding resulted in major NW–SE-trending folds that plunge to the north-west, with an axial planar schistosity. The presence of both rigid rocks (the volcanic pile) and ductile rocks (shale) resulted in disharmonic folding, including north-east-plunging folds, near the base of the sequence (Fig. 3). This deformation can be correlated to the first regional folding phase described above.

The second deformational episode, related to the second regional phase (see above), represents a brittle–ductile shear deformation that produced a number of discrete shear zones. The orientations of these zones are difficult to measure because they have only been recognised in drill core. This style of deformation may be directly related to mercury mineralisation, which appears to occupy one of the zones, possibly subvertical, with a NW–SE orientation, and in conjugate arrangement with the structural zone that controls the Las Cuevas deposits (Palero 1997).

Late Hercynian brittle deformation in this area is represented by NNW–SSE dextral faults. These typically display multiple sets of striations, indicating multistage displacements.

## Mercury mineralisation in the Almadén district

Mercury mineralisation in the Almadén district is of two types: (1) stratabound mineralisation in the Criadero quartzite, possibly introduced shortly after sedimentation, and (2) epigenetic mineralisation, either as veins within quartzite or as massive replacements and stockworks within the volcanic rocks (Hernandez et al. 1999). The deposits of Almadén, El Entredicho and Vieja Concepción are stratabound examples, whereas the Burcio-Tres Hermanas deposit in Devonian quartzites, and the Las Cuevas, Nueva Concepción and Nuevo Entredicho deposits in volcanic rocks represent epigenetic mineralisation.

Both styles of mineralisation contain mono-metallic ore consisting mainly of cinnabar with minor native mercury. Pyrite is also common, especially in epigenetic mineralisation (e.g. Las Cuevas and Nuevo Entredicho deposits). Gangue minerals include quartz, barite, ankerite/dolomite and siderite.

The genesis of both syngenetic and epigenetic ore appears to be related to the presence of the pyroclastic mafic magmatism as stratabound deposits always occur in Criadero quartzite proximal to Frailesca diatremes, and mercury grades decrease away from the contacts (Hernandez 1984). In the epigenetic mineralisation, the bulk of the ore and the highest grades are found in Frailesca rocks because of the combination of two factors: (1) the brittle–ductile deformation in a shear zone that produces local zones of dilation and (2) the reactivity of the secondary


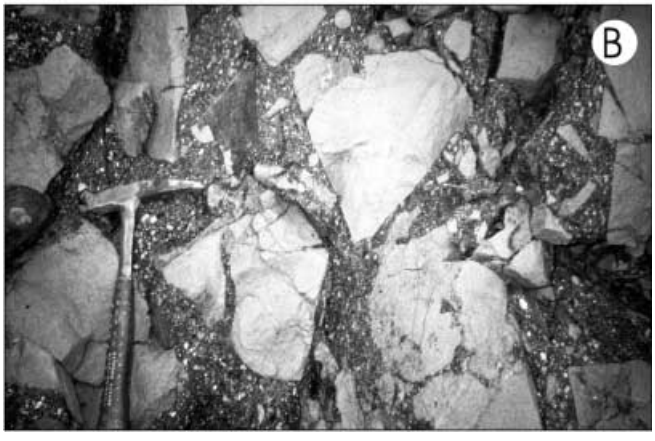


**Fig. 4A, B** Photographs of the ~~Nuevo~~ Entredicho deposit. **A** General view of the diatreme; **B** chaotic breccia composed of prisms of basalt exhibiting cooling textures in a tuffaceous matrix

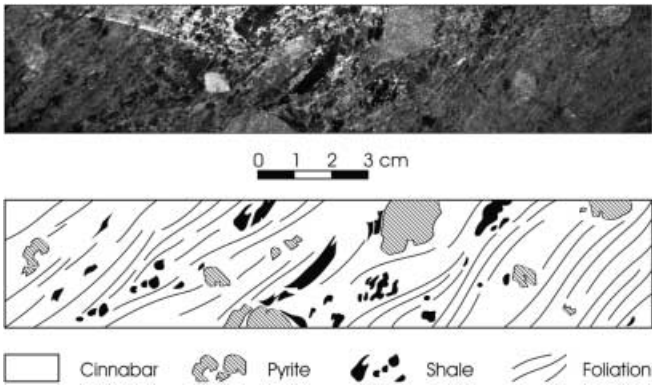


**Fig. 5** Cinnabar-rich sample from a drill-core, Nuevo Entredicho deposit. Cinnabar replacement occurs along a zone of ductile deformation

carbonates with the hot, acid solutions responsible for the epigenetic mineralisation (Higueras 1995; Higueras et al. 1999a).

## Ore at Nuevo Entredicho

Drilling revealed two main types of epigenetic mineralisation in the Nuevo Entredicho area: (1) replacement-style in volcanic tuffs and breccias and (2) cinnabar-bearing veins and tension cracks in sedimentary rocks. The first type always underlies the second due to the geometric position of the respective host rocks.

Replacement-style mineralisation is contained within one horizon only or within two horizons several metres apart, and consists of massive cinnabar replacing Frailesca-type tuffs with graphitic shales as the matrix. The replacement process begins with cement impregnation, followed by total metasomatism of volcanic clasts. Vacuole-rich clasts are more susceptible to replacement than massive clasts, most likely because of their higher permeability. Mineralisation is more intensely developed in strongly foliated zones (Fig. 5), but there is no consistent relationship between plastic deformation and mineralisation. This style of mineralisation is strongly associated with early pyritisation and pyrite-rich layers as thick as 20 cm.

Detailed mineralogical studies using both optical and electronic microscopy revealed that the paragenesis of the replacement-style mineralisation is limited to cinnabar and pyrite; this was subsequently verified by XRD. Two types of pyrite were distinguished: abundant fine-grained framboïdal pyrite, which is typical of diagenesis in black shales, and recrystallised pyrite. Trace-element analyses using laser ablation ICP-MS indicate that the latter can be strongly enriched in copper ($>500$ ppm), lead ($>2{,}000$ ppm) and mercury ($>500$ ppm, with a maximum of 0.4% Hg; Table 1).

Tension-crack mineralisation occurs in black shales and is expressed as 1-cm-thick cracks filled with cinnabar and bounded by small rims of pyrophyllite. Tension cracks display aspect ratios (length/thickness) of approximately twenty. Vein mineralisation typically consists of remobilised dark red cinnabar in small veinlets that cut earlier replacement-style red cinnabar.

Cinnabar samples are very pure, with total trace elements consistently less than 1%. The ICP-MS analyses confirm the presence of some anomalous lead concentrations (172–1,696 ppm; Table 1). Gold and thallium contents are below the detection limits of 5 and 10 ppm, respectively. Minor nickel enrichment (less than 100 ppm) may reflect a local contribution from the mafic rocks in the area.

The concentration of mineralisation along the axis of a regional synclinorium suggests that mercury was emplaced in a low pressure zone during folding and/or shearing. The location of the deposit and the nature of mineralisation and alteration show strong similarities with the ore of the Las Cuevas deposit (Jébrak and Hernandez 1995; Higueras et al. 1999a).

**Table 1** ICP-MS laser ablation analysis on cinnabar and recrystallised pyrite from Nuevo Entredicho deposit, Almadén district, Spain. Analyses performed at BRGM, Orléans, France. All values in ppm

| Sample | Analysis | Mineral | Mineralisation style | Ni | Cu | Pb | Hg |
|---|---|---|---|---|---|---|---|
| 15 | 1 | Pyrite | Tension crack | 18 | 77 | 483 | 3,792 |
| 15 | 2 | Pyrite | Tension crack | 69 | 127 | 498 | 1,612 |
| 15 | 3 | Pyrite | Tension crack | 37 | 260 | 136 | 1,990 |
| 15 | 4 | Pyrite | Tension crack | 19 | 43 | 40 | 523 |
| 15 | 5 | Pyrite | Tension crack | 69 | 191 | 666 | 2,129 |
| 15 | 6 | Pyrite | Tension crack | 70 | 134 | 300 | 2,173 |
| 23 | 1 | Pyrite | Replacement | 16 | 35 | 3,074 | 4,008 |
| 23 | 2 | Pyrite | Replacement | 34 | 877 | 193 | 3,453 |
| 23 | 3 | Pyrite | Replacement | 23 | 92 | 14 | 167 |
| 23 | 4 | Pyrite | Replacement | 32 | 604 | 334 | 600 |
| 23 | 5 | Pyrite | Replacement | 34 | < 10 | 71 | 248 |
| 23 | 6 | Pyrite | Replacement | 17 | 285 | 85 | 227 |
| 14 | 1 | Cinnabar | Tension crack | 86 | < 10 | 650 | |
| 14 | 2 | Cinnabar | Tension crack | 86 | 56 | 897 | |
| 14 | 3 | Cinnabar | Tension crack | 15 | < 10 | 1,002 | |
| 14 | 4 | Cinnabar | Tension crack | 92 | 23 | 1,030 | |
| 14 | 5 | Cinnabar | Tension crack | 83 | 18 | 1,696 | |
| 19 | 1 | Cinnabar | Replacement | 86 | < 10 | 529 | |
| 19 | 2 | Cinnabar | Replacement | 89 | 107 | 172 | |
| 19 | 3 | Cinnabar | Replacement | 66 | 50 | 277 | |
| 19 | 4 | Cinnabar | Replacement | 61 | < 10 | 258 | |
| 19 | 5 | Cinnabar | Replacement | 60 | < 10 | 268 | |
| 30 | 1 | Cinnabar | Replacement | 52 | < 10 | 415 | |
| 30 | 2 | Cinnabar | Replacement | 71 | 21 | 373 | |
| 30 | 3 | Cinnabar | Replacement | 62 | < 10 | 507 | |
| 30 | 4 | Cinnabar | Replacement | 81 | < 10 | 566 | |
| 30 | 5 | Cinnabar | Replacement | 78 | 11 | 734 | |

## Isotopic studies

### Lead isotopes

Lead isotope analyses were performed on five samples of recrystallised pyrite from the Nuevo Entredicho deposit in the BRGM laboratory (Bureau de Recherches Géologiques et Minières, France). Detailed analytical methods are described in Marcoux (1998). Lead extracted from pyrite in mercury-rich assemblages is susceptible to contamination by $^{204}$Hg. For this reason, lead samples were first analysed for $^{202}$Hg to assess the potential for mercury contamination; however, no traces of this metal were found in our samples. Precision was better than 0.01% and reproducibility was 0.12% for $^{206}Pb/^{204}Pb$, 0.16% for $^{207}Pb/^{204}Pb$ and 0.22% for $^{208}Pb/^{204}Pb$. Lead, uranium and thorium values were measured by ICP-MS and are presented in Table 2. Calculated μ ($^{238}U/^{204}Pb$) and W ($^{232}Th/^{204}Pb$) values are very low, ranging from 0.09 to 0.56 and 0.50 to 5.17, respectively. Consequently, corrections for in-situ decay are extremely small. Nevertheless, all values were corrected to 361 Ma (see below).

Lead isotope results are summarised in Table 2. Values are fairly well clustered and characterised by $^{207}Pb/^{204}Pb$ ratios as high as 15.75. There is no difference between pyrites from replacement-style or tension-crack mineralisation. Samples are grouped near the 400 Ma model age isochron (Stacey and Kramers 1975; Fig. 6). Although this model age has no precise geochronological value, it fits well with the illite age recorded at the Las Cuevas and El Entredicho deposits (363–359 Ma; Hall et al. 1997). Despite the high $^{208}Pb/^{204}Pb$ ratios, the elevated $^{207}Pb/^{204}Pb$ ratios in pyrite preclude a contribution from lower continental crust. Instead, the collective lead isotope data strongly suggest a contribution of ancient upper continental crust and do not support a mantle or deep continental crust component for the ores of the Nuevo Entredicho deposit. These isotopic signatures, the first reported for the Almadén district, differ considerably from those of the massive sulphide deposits in the southern Iberian Pyrite Belt for which there is no evidence to support a crustal contribution (Fig. 6; Marcoux 1998).

### Sulphur isotopes

Nine samples of cinnabar and three samples of pyrite were selected for $\delta^{34}S$ analyses (Table 3). Most of the samples came from Nuevo Entredicho drill cores, and the others were collected from the classic stratabound deposit in the El Entredicho open pit for comparison. Sulphur isotope ratios were measured on $SO_2$ gas, produced by sulphide oxidation, using a VG Micromass 602 mass spectrometer at the University of Ottawa. The $\delta^{34}S$ values ($2\sigma = 0.2$ ‰) were standardised to the Canyon Diablo Troilite (CDT).

The results show that the $\delta^{34}S$ signature of cinnabar from Nuevo Entredicho is constant regardless of the mineralisation style (+10.3 to +10.8‰). This suggests

**Table 2** Lead isotopic composition of recrystallised pyrite from the Nuevo Entredicho deposit. Data corrected to 361 Ma. C. Guerrot analyst, BRGM. Pb, U and Th: ICP-MS analyses BRGM, Orléans. $\mu = {}^{238}U/{}^{204}Pb$, $W = {}^{232}Th/{}^{204}Pb$

| Sample | Location | Mineralisation style | $^{206}Pb/^{204}Pb$ | $^{207}Pb/^{204}Pb$ | $^{208}Pb/^{204}Pb$ | Pb (ppm) | U (ppm) | Th (ppm) | μ | W |
|---|---|---|---|---|---|---|---|---|---|---|
| 14 | ME124–126.3 m | Tension crack | 18.352 | 15.753 | 38.604 | 346 | 0.49 | 2.63 | 0.09 | 0.50 |
| 15 | ME124–128.8 m | Tension crack | 18.550 | 15.755 | 38.781 | 44 | 0.34 | 3.40 | 0.50 | 5.17 |
| 18 | ME124–149.8 m | Replacement | 18.386 | 15.748 | 38.594 | 90 | 0.79 | 5.66 | 0.56 | 4.15 |
| 22 | ME142–127.8 m | Replacement | 18.381 | 15.702 | 38.492 | 221 | 0.51 | 4.45 | 0.15 | 1.32 |
| 23 | ME142–175.5 m | Replacement | 18.458 | 15.726 | 38.591 | 157 | 0.49 | 3.50 | 0.20 | 1.47 |

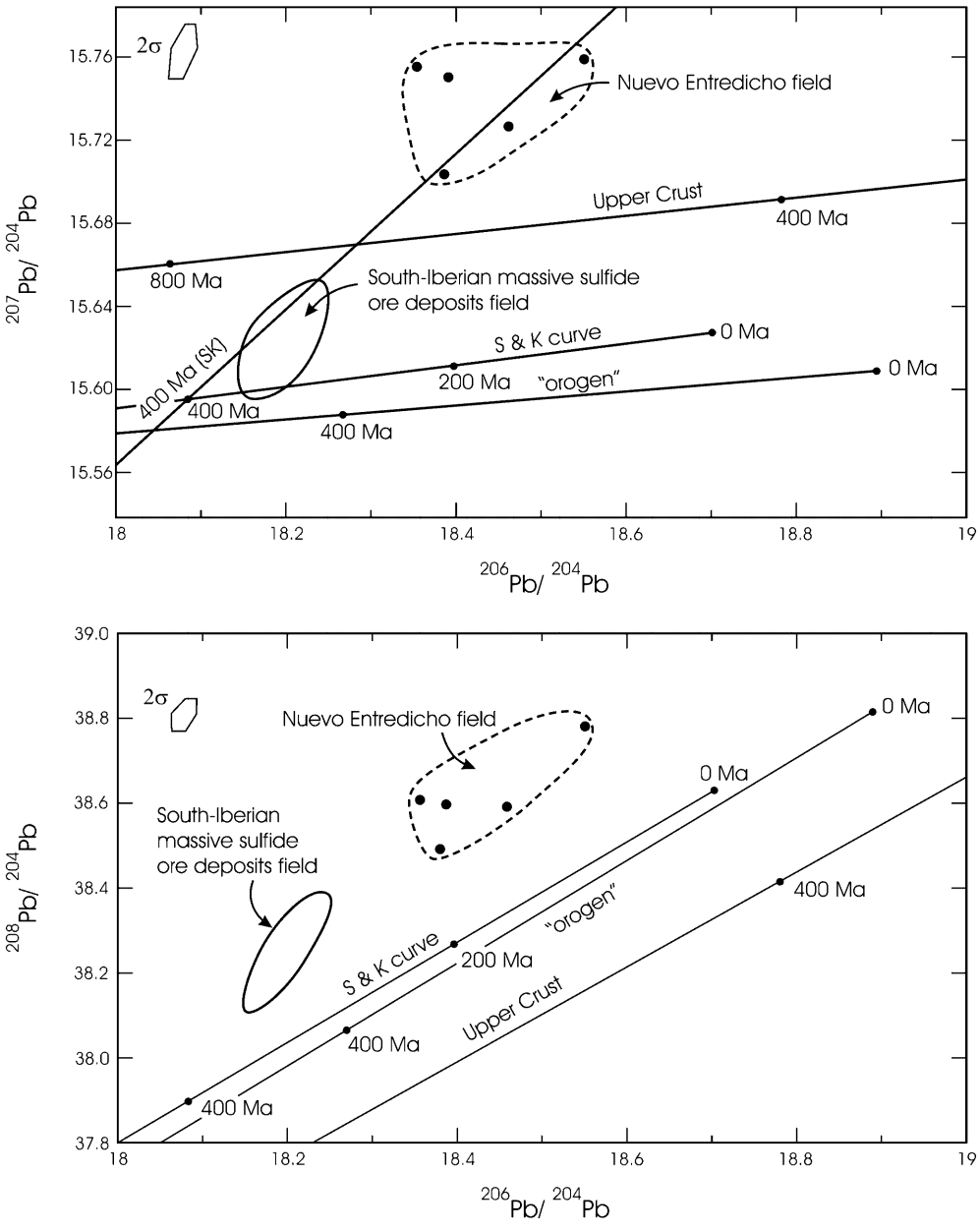


**Fig. 6** Diagrams of $^{206}Pb/^{204}Pb$ versus $^{207}Pb/^{204}Pb$ and $^{206}Pb/^{204}Pb$ versus $^{208}Pb/^{204}Pb$ for recrystallised pyrite of the Nuevo Entredicho deposit. Stacey and Kramer's curve (1975) for crustal lead and the Zartman and Doe curves (1981); '*orogen*' and '*upper-crust*' are shown. Location of the field for massive sulphide ore deposits of the southern Iberian Pyrite Belt is given for comparison (data from Marcoux 1998)

that only one generation of cinnabar is present in the deposit despite the different styles and sites of crystallisation. All the mineralisation was, therefore, formed during the same tectonic episode.

Four samples of cinnabar from the Criadero quartzite of El Entredicho gave more variable $\delta^{34}S$ results, with two analyses of $\sim +1.2‰$ and two of $\sim +7.3‰$ (Table 3). The overall range is similar to that

**Table 3** Sulphur isotope composition at the Nuevo Entredicho (number) and Entredicho (letter) deposits

| Sample | Location | Description | $\delta^{34}$S (‰) Pyrite | $\delta^{34}$S (‰) Cinnabar |
|---|---|---|---|---|
| 14 | ME124–126.3 m | Cinnabar in tension cracks | | 10.3 |
| 18 | ME124–149.8 m | Disseminated cinnabar and recrystallised pyrite, replacement style | 11.9 | 10.8 |
| 19 | ME124–151.5 m | Massive and foliated cinnabar, replacement style | | 10.7 |
| 21 | ME124–181.8 m | Pyrite nodule in graphitic shale | 23.4 | |
| 22 | ME142–127.8 m | Clast replaced by pyrite and cinnabar | 10.6 | |
| 22b | ME142–170.0 m | Massive cinnabar, replacement style | | 10.6 |
| 30 | ME135–108.0 m | Disseminated cinnabar, replacement style | | 10.7 |
| A | ME15–110.2 m | Lower quartzite, disseminated and fracture filling cinnabar (12.6% S) | | 1.4 |
| B | ME24–84.44 m | Lower quartzite, semi-massive cinnabar (38.6% S) | | 7.8 |
| C | ME48–10.50 m | Upper quartzite, cinnabar in fractures (11.8% S) | | 1.0 |
| D | ME48–58.25 m | Lower quartzite, disseminated and fracture-filling cinnabar (33.1% S) | | 6.9 |

for cinnabar samples from the Almadén deposit within the same stratigraphic unit (Saupé and Arnold 1992). These isotopic results correlate strongly with the mercury content of the samples, which is a function of the total sulphur content: low $\delta^{34}$S values characterise low grade mineralisation, whereas high $\delta^{34}$S values are typical of high grade cinnabar ore. This relationship suggests that the sulphur from the samples represents mixing of a low $\delta^{34}$S source, possibly magmatic, with a high $\delta^{34}$S sedimentary source derived from black shales. Organic sulphur in black shales is, on average, about 15‰ lighter than seawater sulphate, which is estimated to be +26 to +31‰ during Ordovician to Silurian time (Claypool et al. 1980; Ohmoto and Goldhaber 1997). The $\delta^{34}$S values for the black shale, therefore, are assumed to be in the +11 to +16‰ range. An increase in the $\delta^{34}$S signature would represent a more significant contribution from the sedimentary sulphur, thus providing a greater availability of sulphur for the cinnabar crystallisation.

In the Nuevo Entredicho deposit, the sulphur isotope signature for volcanic rock-hosted cinnabar is different from that of cinnabar hosted by the stratabound deposits in the Criadero quartzite. The homogeneity of the former indicates a uniform sulphur source for the mineralising fluids or a constant mixing ratio, and constant physicochemical parameters during the formation of the epigenetic deposit. This signature is intermediate between those measured at the epigenetic Las Cuevas deposit (+13‰) and the syngenetic Almadén deposits (0 to +8‰; Fig. 7).

The pyrite analyses, all from the Nuevo Entredicho deposit, comprise two populations, one with $\delta^{34}$S values approximating those of cinnabar (+11.9 and +10.6‰) and another with heavy sulphur (+23.3‰) in black shales. The latter corresponds to diagenetic pyrite. Assuming that isotopic equilibrium was attained, isotope geothermometry using differences in $\delta^{34}$S (~1‰) for one pair of coexisting pyrite and cinnabar samples indicates a temperature of formation of ~300 °C based on the relationship of Ohmoto and Rye (1979). This estimate fits with the temperature range proposed by Saupé (1990) for the Almadén district.

## Discussion

The Nuevo Entredicho deposit was emplaced primarily in a zone of high permeability caused by high porosity in volcanic tuffs affected by carbonatisation, or the presence of tension cracks within black shale. The location of the mineralisation within a fold axis affected by shear deformation and its obvious epigenetic features are indicative of emplacement during a late phase of deformation. This deposit, therefore, displays an obvious resemblance to the Las Cuevas deposit and confirms the existence of volcanic rock-hosted mercury deposits in the Almadén district that lack any association with stratabound pre-concentrations.

Mineralogical and geochemical studies indicate that cinnabar is the only ore mineral produced by the mineralisation process. Pyrite was likely present in the sedimentary rock sequence prior to mineralisation, and was subsequently recrystallised and/or neoformed during cinnabar formation. Investigations of vapour-deposited cinnabar from the California Coast Ranges have shown a marked difference in the purity of this mineral compared with that precipitated from hydrothermal solutions (Rytuba and Heropolis 1992). Vapour-deposited cinnabar contains several tens of ppm of As, Sb, Ag, Cu and Pb in solid solution (zinc content may be higher), and it is common for such cinnabar to contain several hundred ppm of all these metals, including zinc (Barnes and Seward 1997). Therefore, it is likely that the cinnabar of the Nuevo Entredicho deposit, which is enriched in lead, was formed by precipitation from a vapour, most likely steam produced during pyrophyllitic alteration (Hannington 1993). Saupé (1990) dismissed this hypothesis for Almadén because he assumed a submarine environment of mineralisation.

Lead isotope studies on pyrite samples support a metal source derived from old upper continental crust. Successive geological events in such a setting may lead to enriched radiogenic isotopes. These results do not preclude a genetic link with volcanism that could have remobilised part of this old continental crust.

The $\delta^{34}$S values for cinnabar in the volcanic rock-hosted deposits of Nuevo Entredicho and Las Cuevas

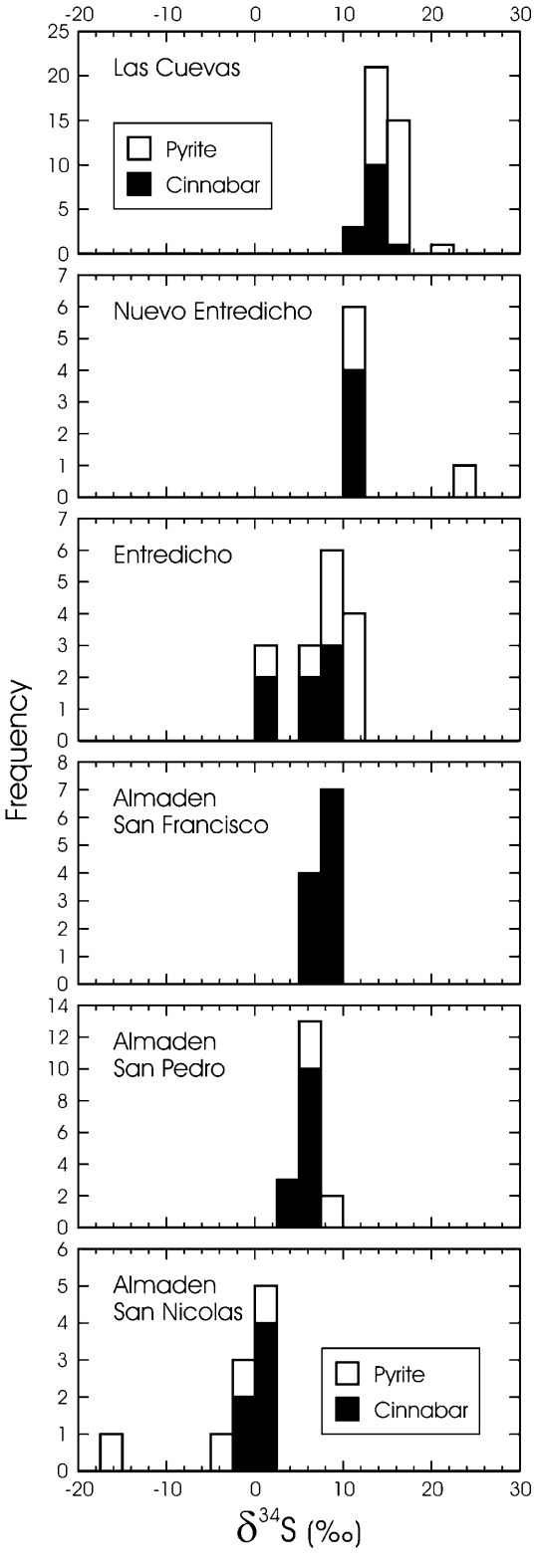


**Fig. 7** Histograms of $\delta^{34}S$ values for cinnabar and pyrite from mercury deposits of the Almadén district. Stratabound mineralisation: Almadén (Saupé and Arnold 1992), Entredicho (Rytuba et al. 1989; this study); Epigenetic mineralisation: Nuevo Entredicho (this study) and Las Cuevas (Rytuba et al. 1989; Higueras et al. 1999b)

are higher than those measured in sedimentary rock-hosted deposits such as Almadén (Table 4, Fig. 7). The different mineralisation styles of the district are characterised by specific $\delta^{34}S$ values (Higueras et al. 1999b), which implies that each deposit of the Almadén district was related to a different hydrothermal system. The $\delta^{34}S$ values of approximately $+10‰$ in cinnabar and associated pyrite could not be produced by a magmatic fluid, nor by a direct leaching of footwall shales ($\delta^{34}S = +5.5‰$) or spilites ($\delta^{34}S = +5.1‰$), as suggested by Saupé and Arnold (1992) for the Almadén deposit. These hypotheses should, therefore, not be applied to the volcanic rock-hosted deposits.

The variable $\delta^{34}S$ signatures at a regional scale may signify that different chemical conditions for mercury deposition existed in each deposit (e.g. $fO_2$, $fS$, pH parameters, duration of wall rock interactions; Ohmoto and Rye 1979), or that there were different sulphur sources. Mineral assemblages, however, do not indicate any significant temperature variations. One possible scenario to explain the isotopic variations between deposits requires remobilisation of sedimentary sulphur in a convective hydrothermal system. The shift in $\delta^{34}S$ signature between a possible source of sedimentary sulphur in stratabound ore at El Entredicho (Rytuba et al. 1989; Higueras et al. 1999b) and the site of deposition in Nuevo Entredicho was calculated to be $8.4 \pm 0.8‰$. This difference would increase with increasing $SO_4^{2-}/H_2S$ ratios in the fluid (Ohmoto and Rye 1979), suggesting that highly reducing conditions existed at Nuevo Entredicho. The abundance of sulphide minerals and the high grade cinnabar ore in the Nuevo Entredicho deposit suggest a sulphide-rich fluid with a high sulphide/sulphate ratio during mercury mobilisation.

## Conclusions

The Nuevo Entredicho deposit contains the richest concentration of mercury in the Almadén district. It is located within an alkaline diatreme where volcanic rock deposition is dominated by juvenile magmatic tephra and lithic fragments within a water-saturated media. The abundant vacuoles in the basaltic rocks and the early precipitation of calcite probably signify early $CO_2$ degassing. Emplacement of the diatreme was almost synchronous with the deposition of the Criadero quartzite, which hosts the bulk of the district's mercury mineralisation.

The Nuevo Entredicho deposit is characterised by volcanic rock-hosted mineralisation that displays epigenetic characteristics and a pyrophyllite alteration zone, similar to those described elsewhere by Sillitoe et al. (1996). Compared with the world-class Almadén deposit, Nuevo Entredicho is of smaller size and has similar metal associations, but has higher grade ore and contains cinnabar characterised by heavier $\delta^{34}S$ signatures. Lead isotope measurements for pyrite suggest that the mineralisation was initially derived from old

**Table 4** Comparison between sulphur isotope data of cinnabar from various deposits in the Almadén mercury district

| Deposit | Type | $\delta^{34}S$ (‰) | Sample number | Reference |
|---|---|---|---|---|
| Almadén–San Nicolas | Stratabound | $0.2 \pm 1.1$ | 6 | Saupé and Arnold (1992) |
| Almadén–San Pedro | Stratabound | $5.9 \pm 1.0$ | 13 | Saupé and Arnold (1992) |
| Almadén–San Francisco | Stratabound | $8.1 \pm 0.7$ | 11 | Saupé and Arnold (1992) |
| El Entredicho | Stratabound | $8.0 \pm 1.0$ | 5 | Rytuba et al. (1989); this study |
| El Entredicho | Stratabound | $1.2 \pm 0.3$ | 2 | This study |
| Nuevo Entredicho | Epigenetic | $10.6 \pm 0.2$ | 5 | This study |
| Las Cuevas | Epigenetic | $13.3 \pm 1.0$ | 13 | Rytuba et al. (1989); Higueras et al. (1999b) |

continental crust, and subsequently remobilised during Devonian volcanism and Hercynian deformation.

This study shows that grade variations in the Almadén district are related to two main factors. Firstly, volcanic rock-hosted mercury deposits, such as Nuevo Entredicho and Las Cuevas, display higher mercury grades than sedimentary rock-hosted deposits. The former reaches grades as high as 50–60%, with more typical values of about 25%, whereas those of quartzite deposits attain maximum grades of 10–12%. This higher grade is partly related to reactivity with carbonatised host rocks, and partly to tectonic concentration in tension cracks in the highly-deformed low pressure zones of sheared and/or folded structures. Secondly, the Nuevo Entredicho deposit is also of higher grade because abundant reducing black shale increased the efficiency of the precipitation process during destabilisation of metal-carrying complexes.

**Acknowledgements** This paper is a contribution to IGCP Project 427 (Ore-forming processes in dynamic magmatic systems). M. Auclair and V. Bodycomb are thanked for editing the manuscript, and M. Laithier for the figures. The comments of F. Saupé, R.J. Goldfarb and one anonymous reviewer greatly improved the quality of the final manuscript.

## References

Aranda-Gómez JJ, Luhr JF (1996) Origin of the Joya Honda maar, San Luis Potosí, Mexico. J Volcanol Geotherm Res 74:1–18

Barnes HL, Seward TM (1997) Geothermal systems and mercury deposits. In: Barnes HL (ed) Geochemistry of hydrothermal ore deposits, 3rd edn. Wiley, Chichester, pp 699–736

Boxer GL, Jaques AL (1990) Argyle (AK1) Diamond deposit. In: Hughes FE (ed) Geology of the mineral deposits of Australia and Papua New Guinea, vol 1. Australasian Institute Mining Metallurgy, Monograph no 14, Melbourne, pp 697–706

Cas RAF (1989) Physical volcanology; explosive eruption centres. In: Johnson RW, Knutson J, Taylor SR (eds) Intraplate volcanism in eastern Australia and New Zealand. Cambridge University Press, Cambridge, pp 78–83

Claypool GE, Holser WT, Kaplan IR, Sakai H, Zak I (1980) The age curves of sulphur and oxygen isotopes in marine sulfate and their mutual interpretation. Chem Geol 28: 199–260

Dallmeyer RD, Martinez Garcia E (1990) Pre-Mesozoic geology of Iberia. Springer, Berlin Heidelberg New York

Gallardo JL, Higueras P, Molina JM (1994) Análisis estratigráfico de la 'Cuarcita de Criadero' en el sinclinal de Almadén. Bol Geol Minero 105(2): 135–145

Garcia Sansegundo JI, Lorenzo Alvarez S, Ortega E (1987) Mapa Geologico Nacional a escale 1:50,000, sheet no 808 (Almadén), Institute of Geology, Minero Esp., Madrid

Hall CM, Higueras P, Kesler SE, Lunar R, Dong H, Halliday AN (1997) Dating of alteration episodes related to mercury mineralisation in the Almadén district, Spain. Earth Planet Sci Lett 148: 287–298

Hannington MD (1993) Shallow submarine hydrothermal systems in modern island arc settings. Gangue 43: 6–9

Hernandez A (1984) Estructura y génesis de los yacimientos de mercurio de la zona de Almadén. PhD Thesis, University de Salamanca

Hernandez A, Jébrak M., Higueras P, Oyarzun R, Morata D, Munhà J (1999) The Almadén mercury mining district, Spain. Miner Deposita 34: 539–548

Higueras P (1995) Procesos petrogenéticos y de alteración de las rocas magmáticas asociadas a las mineralizaciones de mercurio del distrito de Almadén. PhD Thesis, Universidad de Granada, Ediciones de la Universidad de Castilla-La Mancha, Cuenca

Higueras P, Munhá J (1993) Geochemical constraints on the petrogenesis of mafic magmas in the Almadén mercury mining district. Terra Abstr 5: 12–13

Higueras P, Oyarzun R, Lunar R, Sierra J, Parras J (1999a) The Las Cuevas deposit, Almadén district (Spain): a unusual case of deep-seated advanced argillic alteration related to mercury mineralization. Miner Deposita 34: 211–214

Higueras P, Saupé F, Tena JC (1999b) Episodios de mineralización únicos en los yacimientos epigenéticos de mercurio de Almadén: evidencias isotópicas en el yacimiento de Las Cuevas. Geogaceta 25: 107–109

Higueras P, Oyarzun R, Munhá J, Morata D (2000). The Almadén metallogenetic cluster (Ciudad Real, Spain): alkaline magmatism leading to mineralization process at an intraplate tectonic setting. Rev Soc Geol Esp 13(1): 105–119

Higueras P, Oyarzun R, Munhá J, Morata D (2001) Paleozoic magmatic-related hydrothermal activity in the Almadén syncline (Spain): a Silurian–Devonian persistent process? Trans Inst Min Metall 109: B199–B202

Jébrak M, Hernandez A (1995) Tectonic deposition of mercury in the Almadén district (Las Cuevas deposit, Ciudad Real, Spain). Miner Deposita 30: 413–423

Jébrak M, Hernandez A (1997) Tectonic deposition of mercury in the Almadén district (Las Cuevas deposit, Ciudad Real, Spain). A reply. Miner Deposita 32: 299–300

Julivert M, Fontboté JM, Ribeiro A, Conde LEN (1972) Mapa tectónico de la peninsula Ibérica y Baleares a escala 1:1,000,000, Institute of Geology, Minero. Esp., Madrid

Marcoux É (1998) Lead isotope systematics of the giant massive sulphide deposits in the Iberian pyrite belt. Miner Deposita 33: 45–58

Nägler TF, Schäfer HJ, Gebauer D (1992) A Sm–Nd isochron on pelites 1 Ga in excess of their depositional age and its possible significance. Geochim Cosmochim Acta 56: 789–795

Ohmoto H, Goldhaber MG (1997) Sulfur and carbon isotopes. In: Barnes HL (ed) Geochemistry of hydrothermal ore deposits, 3rd edn. Wiley, Chichester, pp 517–600

Ohmoto H, Rye RO (1979) Isotopes of sulfur and carbon. In: Barnes HL (ed) Geochemistry of hydrothermal ore deposits, 2nd edn. Wiley, Chichester, pp 509–567

Ortega E (1997) Comments on the paper by M. Jébrak and A. Hernandez: tectonic deposition of mercury in the Almadén

district, Las Cuevas Deposit, Spain. Miner Deposita 30: 413–423 (1995). Miner Deposita 32: 296–298
Palero F (1997) A tectonic reinterpretation of Las Cuevas deposit. Internal report. Minas de Almadén
Prado del C (1855) Sur la géologie d'Almadén, d'une partie de la Sierra Morena et des montagnes de Toledo. Bull Soc Geol Fr (2ème Série) 12: 182–204
Rytuba JJ, Heropolos C (1992) Mercury – an important byproduct in epithermal gold systems. In: De Young JH, Hammarstrom JM (eds) Contributions to commodity geology research. US Geol Surv Bull 1877, pp D1–D8
Rytuba JJ, Rye RO, Hernandez AM, Dean JA, Arribas A Sr (1989) Genesis of Almadén type mercury deposits, Almadén, Spain, vol 2. International Geology Congress, Washington
Saupé F (1973) La géologie du gisement de mercure d'Almadén (Province de Ciudad Real, Espagne). Sciences de la Terre, Mémoire 29
Saupé F (1990) Geology of the Almadén mercury deposit, Province of Ciudad Real, Spain. Econ Geol 85: 482–510
Saupé F, Arnold M (1992) Sulphur isotope geochemistry of the ores and country rocks at the Almadén mercury deposit, Ciudad Real, Spain. Geochim Cosmochim Acta 56: 3765–3780
Shelley D, Bossière G (2000) A new model for the Hercynian Orogen of Gondwana France and Iberia. J Struct Geol 22: 757–776
Sillitoe RH, Hannington MD, Thompson JFH (1996) High sulfidation deposits in the volcanogenic massive sulfide environment. Econ Geol 91: 204–212
Stacey JS, Kramers JD (1975) Approximation of terrestrial lead isotope evolution by a two-stage model. Earth Planet Sci Lett 26: 207–221
Thorarinsson S (1967) Some problems of volcanism in Iceland. Geol Rundsch 57: 1–20
Van der Veen RW (1924) The Almadén mercury ores and their connection with igneous rocks. Econ Geol 29: 146–156
Villas E, Lorenzo S, Gutiérrez-Marco JC (1999) First record of a *Hirnantia* Fauna from Spain, and its contribution to the Late Ordovician palaeogeography of northern Gondwana. Trans R Soc Edinb Earth Sci 89: 187–197
Zartman RE, Doe BR (1981) Plumbotectonics – the model. Tectonophysics 75: 135–162